Environ. Sci., Hokkaido	6 (2)	301~317	Dec. 1983

Air Current System in Hokkaido

—An Analysis Using Wind Vector Composition Method—

Hisashi Kato

Energy and Environment Laboratory, Environment Department, Atmospheric Environment Section, Central Research Institute of Electric Power Industry, Tokyo 201

北 海 道 の 気 流 系

——風ベクトル合成法による解析——

加 藤 央 之

電力中央研究所エネルギー研究所環境部大気環境研究室

1. Introduction

In the previous paper (Kato, 1982) it was pointed out that the clear air current in any general wind direction should be described in order to clarify the regional features of wind. Then in this paper the regional characteristics of air current are described in detail by means of an original method developed by the author.

Since the wind is a vector, its treatment is difficult. PCA (Principal component analysis) has been applied to wind data in a few studies. Barnett (1977) showed the wind distribution patterns for u and v components, respectively. This procedure is also used by Wakamatsu and Hatano (1981) and Enfield (1981). On the other hand, Hardy (1978) showed the wind distribution pattern as analysed from the vector component. However, the former studies did not show the actual air current systems and the latter showed only a few air current systems.

Then in order to clarify the various features of air current systems the following methods are used. (1) The u and v components are analysed by PCA, respectively. (2) Distribution patterns of u and v components are calculated using the results of (1) when the corresponding Z-score has the maximum or the minimum value. (3) Each distribution pattern of $u\,(v)$ component is combined with that of each $v\,(u)$ component referring to the correlation between Z-scores of u and v components. (4) The air current systems are described using the results of (3). (5) Pressure patterns corresponding to the systems are investigated. The air current systems constructed by this method indicate the wind distribution pattern when

Received 8 Oct. 1983
1983年10月8日受理

the general wind speed is strong in each direction.

2. Data and Methods

In this analysis the AMeDAS (Automated Meteorological Data Acquisition System) wind data in 1978 are used. Basic data for $u\,(v)$ component (134 stations $\times$ 365 days), for example the $u\,(v)$ axis corresponding to E-W (N-S) direction, are obtained from the daily mean of $u\,(v)$ component at each station. Missing data which are interpolated by the three neighboring stations by the method of Suzuki (1964) are 0.66% of the total data and are regarded not to affect the results in this analysis.

For the sake of brevity, the case with two variables is treated in the following explanation. If we plot the wind data of each day on an orthogonal coordinate system, O-xy, with U_1 (daily u component at one station) as x coordinate axis and with U_2 (daily u component at another station) as y coordinate axis, the points on the plane are scattered in a elliptical fashion (Fig. 1). In order to inspect the relation between U_1 and U_2, principal component Z_{1u} (first component) and Z_{2u} (second component) are calculated. Hence the character u indicates u component. These principal components are given by

$$Z_{1u} = l_{11} \cdot U_1 + l_{12} \cdot U_2 \qquad (1)$$

$$Z_{2u} = l_{21} \cdot U_1 + l_{22} \cdot U_2\,, \qquad (2)$$

where l_{ij} is the coefficient of the equations. These principal components indicate the rotation of the orthogonal coordinate system and are defined by

$$Z_{1u} = U_1 \cdot \cos\theta + U_2 \cdot \sin\theta \qquad (3)$$

$$Z_{2u} = -U_1 \cdot \sin\theta + U_2 \cdot \cos\theta \qquad (4)$$

The direction of Z_{1u} is in agreement with that of the apse line and also Z_{2u} with the minor axis. It is clear that the increase (decrease) of Z_{1u} shows the increase (decrease) both of U_1 and U_2 (see Fig. 1). Similarly, the increase (decrease) of

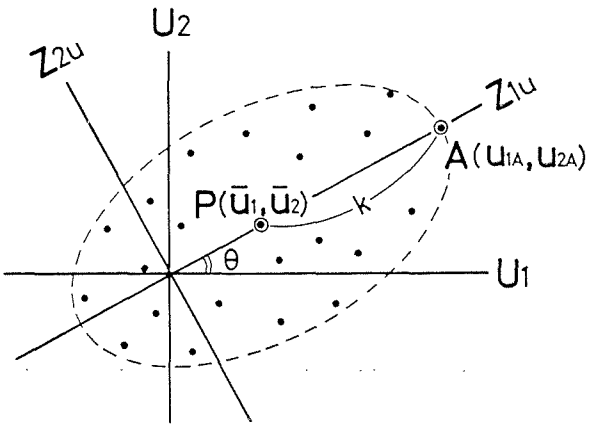

Fig. 1. An explanation of PCA in the case with two variables.

Z_{2u} shows both the decrease (increase) of U_1 and increase (decrease) of U_2. The data of the day when Z_{1u} has the maximum value corresponds to point A in Fig. 1. As is evident from the figure, U_1 and U_2 values of this day, i. e. U_{1A} and U_{2A}, are written as

$$U_{1A} = U_1 + k \cdot \cos\theta \tag{5}$$

$$U_{2A} = U_2 + k \cdot \sin\theta \tag{6}$$

where U_1 (U_2) is the annual mean of U_1 (U_2). Substituting (5) and (6) in (3), one obtains

$$Z_{1u\cdot\max} = U_1 \cdot \cos\theta + U_2 \cdot \sin\theta + k \tag{7}$$

where $Z_{1u\cdot\max}$ shows the maximum value of Z_{1u} during the year. In the equation (7), $\bar{U}_1$ and $\bar{U}_2$ are calculated from the data. The values of $\cos\theta$ ($=l_{11}$) and $\sin\theta$ ($=l_{12}$) are also obtained as a result of PCA. Since the total of the first two terms in the right side of equation (7) equals the annual mean of Z_{1u}, Z_{1u} is used in the actual calculation. If the $Z_{1u\cdot\max}$ is obtained, the value of k is determined. Thus, substituting the k value into (5) and (6), one obtains U_{1A} and U_{2A}. In this analysis Z_{1u}-score is calculated for each day using equation (1), and its frequency is approximately regarded as Normal distribution. $Z_{1u\cdot\max}$ is determined from the distribution as the value which occurs once a year.

In much the same manner as this, u components of two stations corresponding to the minimum score of Z_{1u}, and to the maximum and minimum scores of Z_{2u} are calculated. One also obtains the v components to each Z-score. These procedures are applicable in a case with a large number of variables. When the number of variables is n, u or v components at each station are all calculated corresponding to the maximum and minimum values of Z_{iu} ($i=1, ,2 ,\cdots, n$) and Z_{ju} ($j=1, 2, \cdots, n$), respectively.

Next, the coefficients of correlation between Z_{ju} and Z_{jv} are calculated and the couples with high correlations are picked up. For example, we assume that the correlation between Z_{1u} and Z_{2v} has a high positive value in the case of two variables. Since the time variations of Z_{1u} and Z_{2v} are similar to each other, Z_{2v} is apt to be close to its maximum value when Z_{1u} has its maximum value. In other words the distribution of u component, U_{11} and U_{12} (at $Z_{1u\cdot\max}$), tends to occur when the v component has the distribution pattern of V_{21} and V_{22}, corresponding to $Z_{2v\cdot\max}$. Hence the affixed numbers of $U(V)$ indicate the order of principal component (former) and the station number (latter). Then based on the assumption that both $Z_{1u\cdot\max}$ and $Z_{2v\cdot\max}$ occur at the same time, the wind at each ith station at that time is obtained by composing the vector components U_{1i} and V_{2i}. This procedure can be applied in general cases (p-variables) (see Fig. 2). The wind distribution patterns obtained by these procedures are discussed in connection with the pressure patterns.

By these methods, wind distribution patterns determined by synoptic scale pressure field and the major topographical features alone can be delineated, and the

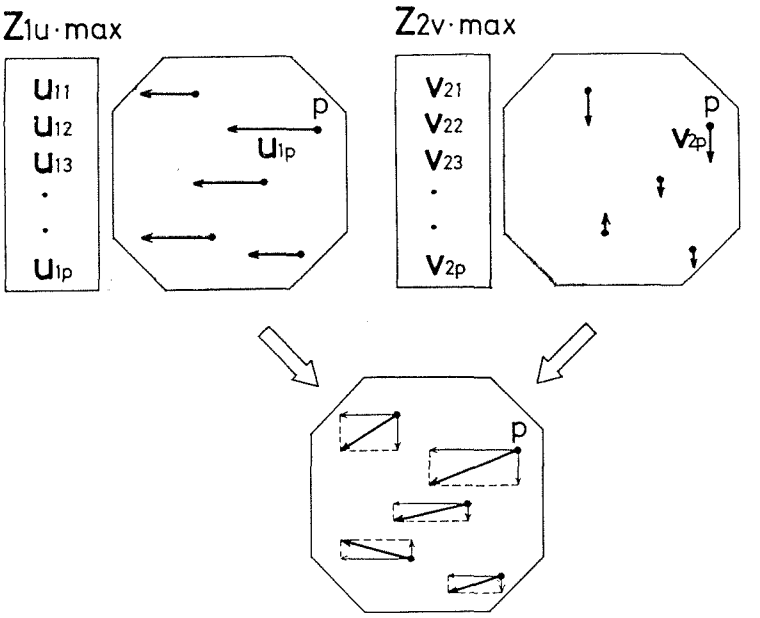

Fig. 2. A schema for composing vector components. See the text for detail.

noise such as background fluctuation of wind peculiar to each station or the wind related to the heat effect is removed. This is the outstanding merit of these methods.

3. Analysis

The proportions of each principal component on the case of 1) u(E-W) and v(N-S) and 2) u(SE-NW) and v(NE-SW) are shown in Table 1. The accumulated proportion of the first two principal components exceeds by about 70% in both cases of 1) and 2).

Fig. 3 shows an example for the frequencies of Z_{1u}- and Z_{1v}-scores in the case when u and v axes correspond to the E-W and N-S lines, respectively. In

Table 1. Proportions of first five principal components in the case of 1) u(E-W)-v(N-S) axes and 2) u(SE-NW)-v(NE-SW) axes (%)

	1	2	3	4	5
1)					
u-component (E-W)	56.6	13.8	5.9	3.6	2.6
v-component (N-S)	62.4	9.1	6.1	2.7	2.3
2)					
u-component (SE-NW)	64.9	9.8	4.2	3.4	2.2
v-component (NE-SW)	52.1	14.1	7.0	4.2	2.9

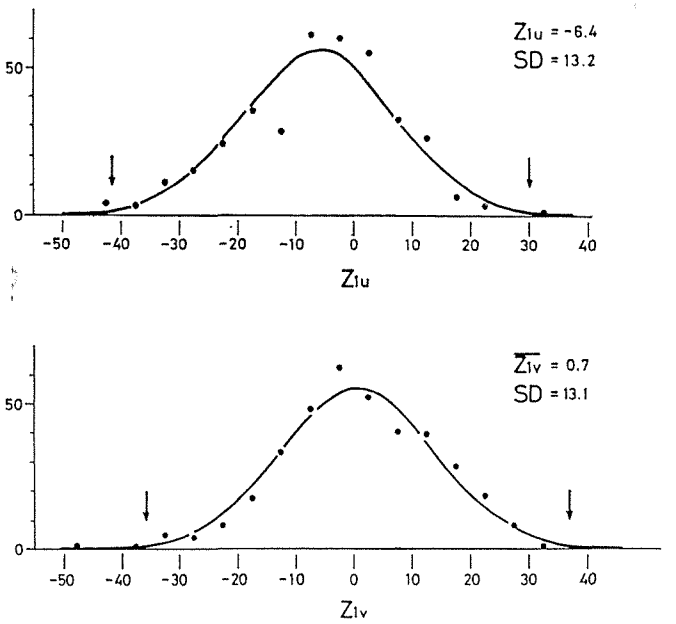

Fig. 3. Frequencies of Z_{1u} and Z_{1v} for the case with u-component along E-W direction. Dot shows each frequency. The curves show the Normal distribution derived from the mean and the standard deviation for each Z-score. Arrows indicate the maximum and the minimum Z-scores determined from each Normal distribution.

the figure the abscissa corresponds to the Z-score and ordinate to the frequency. Dots indicate each frequency and the curve of the Normal distribution is described by the mean and the standard deviation in each Z-score. Since the distributions of Z-scores are similar to the calculated curves including these cases, each maximum (minimum) Z-score is determined from these Normal distributions as they occur once a year (i. e., about 0.27% of the total data). These are shown by arrows in the figures. Then the distributions of u and v components are calculated at each maximum and minimum value by the equations (5), (6) and (7).

The correlation between Z_{iu} $(i=1, 2, \cdots, 5)$ and Z_{jv} $(j=1, 2, \cdots, 5)$ for the two cases 1) and 2) mentioned above are shown in Table 2. A positive or negative correlation clearly exists between Z_{1u} and Z_{2v}, and between Z_{1v} and Z_{2u} in both cases 1) and 2). Then the u and v components corresponding to the extreme Z-scores are combined at each station (see Fig. 2), and the wind distribution patterns are obtained. In each direction, the score of Z_{1u} (Z_{1v}) is highly correlative (greater than 0.98) to the areal mean of daily $u(v)$ component. Namely, the Z_{1u} (Z_{1v})-score shows the strength of the areal mean wind speed with regard to the direction of $u(v)$ component, and the wind pattern corresponding to $Z_{1u\cdot\max}$ $(Z_{1v\cdot\max})$ appears when the areal mean of daily $u(v)$ component shows a maximum value. In the case of u(E-W) and v(N-S), with the east direction as the positive, the wind pattern corresponding to $Z_{1u\cdot\max}$ shows the air current system when the

Table 2. Correlation coefficients between first five Z-scores of u(E-W) and v(N-S) components

1) u(E-W), v(N-S)

	Z_{1v}	Z_{2v}	Z_{3v}	Z_{4v}	Z_{5v}
Z_{1u}	0.37	−0.83	−0.14	0.02	−0.18
Z_{2u}	0.78	0.30	0.19	0.04	0.06
Z_{3u}	−0.27	−0.11	0.11	0.14	0.20
Z_{4u}	−0.28	−0.05	−0.04	−0.12	−0.12
Z_{5u}	0.05	0.12	−0.42	0.11	0.27

2) u(SE-NW), v(NE-SW)

	Z_{1v}	Z_{2v}	Z_{3v}	Z_{4v}	Z_{5v}
Z_{1u}	−0.10	−0.90	−0.15	−0.21	−0.04
Z_{2u}	−0.78	0.13	−0.31	−0.05	−0.07
Z_{3u}	−0.24	−0.13	−0.03	0.45	0.13
Z_{4u}	0.07	−00.9	0.03	0.11	−0.03
Z_{5u}	0.32	0.01	−0.22	−0.14	−0.22

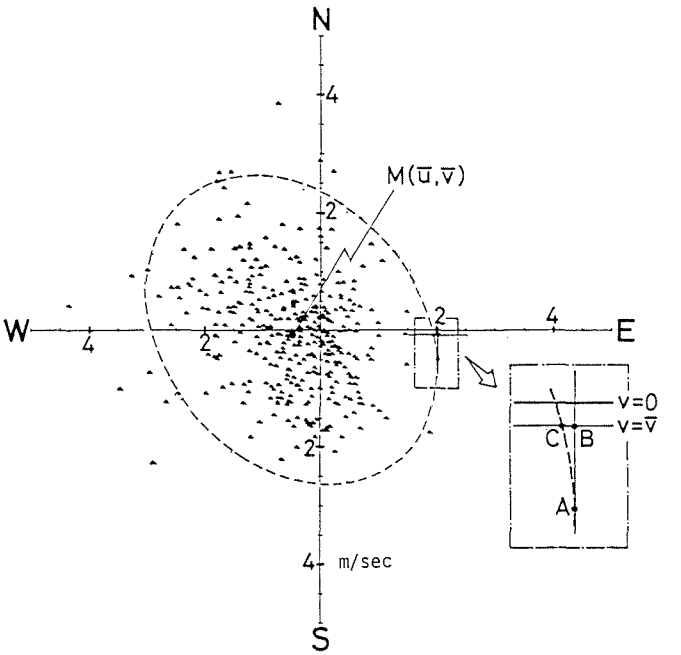

Fig. 4. Areal mean vector wind for each day (1978). Broken line indicates the maximum wind speed calculated for each direction. See Section III-4-c for the discussion.

easterly component of areal mean wind has the maximum value. On the other hand, the pattern at $Z_{1u\cdot\min}$ describes that for the westerly winds.

Furthermore, the areal mean vector wind when each Z-score has extreme value is examined. The areal mean vector wind for each day (1978) is shown in Fig. 4. The dashed line indicates the maximum wind speed for each direction calculated in the same manner as in the case of Fig. 3. Hence, point A (in the rectangle surrounded by dashed dotted lines) shows the maximum value of the areal mean u component (easterly wind), and corresponds to $Z_{1u\cdot\max}$. However, when Z_{1u} has a maximum value, it is assumed that $Z_{2v} \fallingdotseq Z_{2v\cdot\max}$ and $Z_{1v} \fallingdotseq \overline{Z_{1v}}$, i. e., $v \fallingdotseq \bar{v}$. Namely, the wind distribution pattern at $Z_{1u} = Z_{1u\cdot\max}$ obtained here is actually that at point B ($u \fallingdotseq u\cdot\max$ and $v \fallingdotseq \bar{v}$). In the figure, as the maximum value is that of point C, the pattern at point B shows that under a slightly stronger wind speed than the measured one. Although the errors actually exist as in this case, their influences seem to be very small in this analysis. Then, each wind distribution pattern obtained here is considered to be that when the areal mean vector wind in each direction has the maximum wind speed of the year, although some errors are present in some cases

Table 3 shows the relation between the direction of areal mean vector wind

Table 3. Relation between the areal mean vector wind and the pressure gradient with direction in the case when the areal mean wind speed is greater than 1.0 m/sec. The value in the table indicates the frequency of each wind data. The direction of pressure gradient (e. g. 16; the pressure is higher in the northern side) is calculated from the data of Wakkanai, Hakodate and Nemuro

AVERAGE WIND DIRECTION	DIRECTION OF PRESSURE GRADIENT															
	1	2	3	4 E	5	6	7	8 S	9	10	11	12 W	13	14	15	16 N
1															2	
2															1	2
3																
4 E		2	2													
5			2													
6				4	1											
7				5	8											
8 S					2	17	3									
9						1	11	7	1							
10							5	6	5							
11								4	12							
12 W									15	5						
13									1	22	12					
14										1	12	11	1			
15												3	4	4		
16 N														5	3	

and the direction of the pressure gradient calculated from the sea level pressure of Wakkanai, Hakodate and Nemuro in the case when the areal mean wind speed is greater than 1.0 m/sec. The value in the table indicates the frequency of each wind. From the table, it is noted that the direction of areal mean wind is rotated counterclockwise about one direction (i. e. 22.5°) from that of the gradient wind estimated from the pressure gradient, and is actually similar to the direction of general wind. Thus the areal mean wind is regarded as the general wind in this analysis. Ultimately, air current systems obtained here correspond to the wind pattern when the general wind speed in each direction has the annual maximum value.

4. Results and Discussions

a. Air current system

The air current systems when the general wind speed has the annual maximum value in each direction are shown in Figs. 5 (a)-(h). Each general wind direction is shown on the upper part of the figure. Thick solid arrows correspond to the wind speed over 5 m/sec and dashed arrows to that under 1 m/sec.

Generally speaking, each air current system seems to be determined both by the general wind direction and the major topographic features as pointed out by Kawamura (1963, 1966). Referring to the wind speed, strong wind areas exist along the airways. On the other hand the weak wind areas lie to the leeward of obstructions such as mountains.

Figs. 5 (a)-(h) correspond to Fig. 3 of Kawamura (1963). Both figures show air current systems under strong general wind. However, since the definition of general wind direction in this study has some differences from that of Kawamura (1963), such figures can not be compared simply. For example, Fig. 5 (g) corresponds to the case under general wind direction between W and NW in his study. Furthermore, the data using in this analysis (daily mean) is also different from those of his study (wind at 0900 (JST)). Although some differences exist between these two studies, both figures show analogous features regarding some air current systems. Each map of Fig. 5 seems to compensate for the features in some general wind directions between those of Kawamura (1963).

Then including further discussions of the properties of these results, the features of air current in several areas are investigated in the following.

1) Ishikari Lowland (Ishikari Plain-Yūfutsu Lowland)

The distinct air current exists in the area under the southerly or northerly general wind. Especially under the southerly general wind, it is also characterized that the stream line is divided by the Mashike Mountains as mentioned by Owada and Yoshino (1971) which are the same as the features clarified in the previous paper (Kato, 1982). One of these air currents toward Ishikari Plain clearly exist under southeasterly or southerly general winds, on the other hand another exists under the southerly or southwesterly general wind.

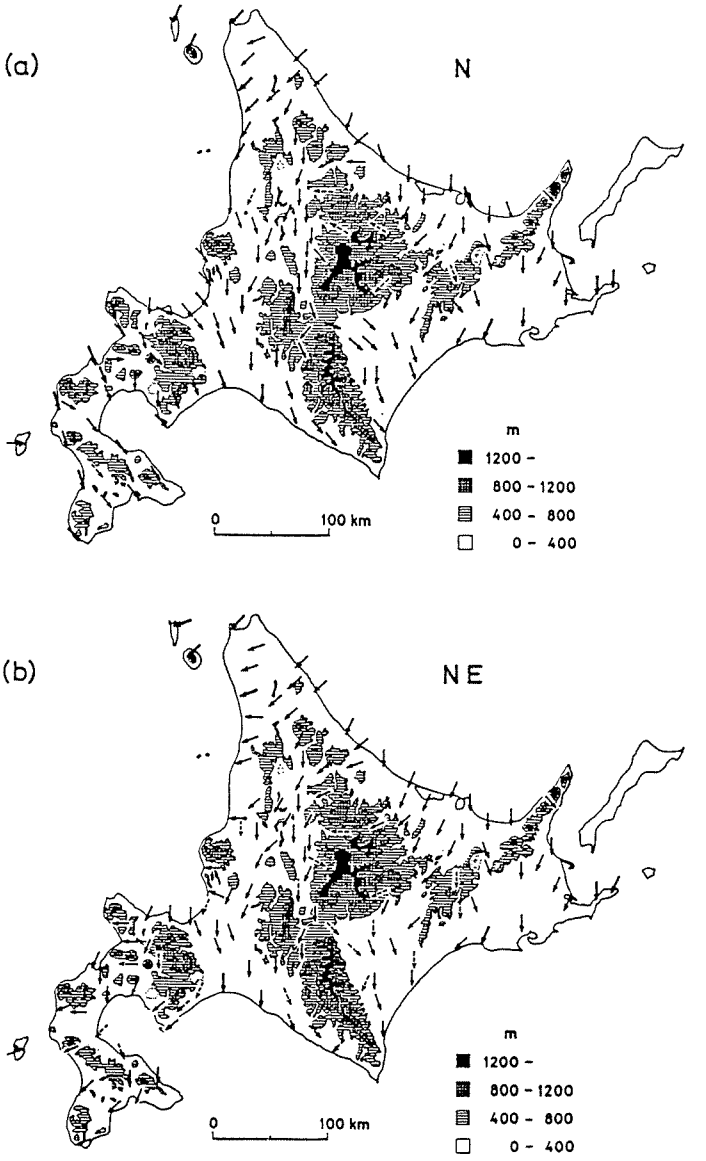

Fig. 5. (a) Air current map for northerly general wind with maximum wind speed for the direction during a year. Thick solid arrows correspond to the wind speed over 5 m/sec and broken arrows to that under 1 m/sec. (b) Same as (a), except for northeasterly general wind.

Under the southwesterly general wind westerly surface wind exists to the north of the Ishikari Bay. The area of westerly surface wind seems to extend from the northern Japan Sea side to the south as the general wind direction turns from S to NW (see Figs. 5 (e)-(h)). This phenomenon appears both by the change of general wind direction and by the influence of Shiribeshi Mountains which

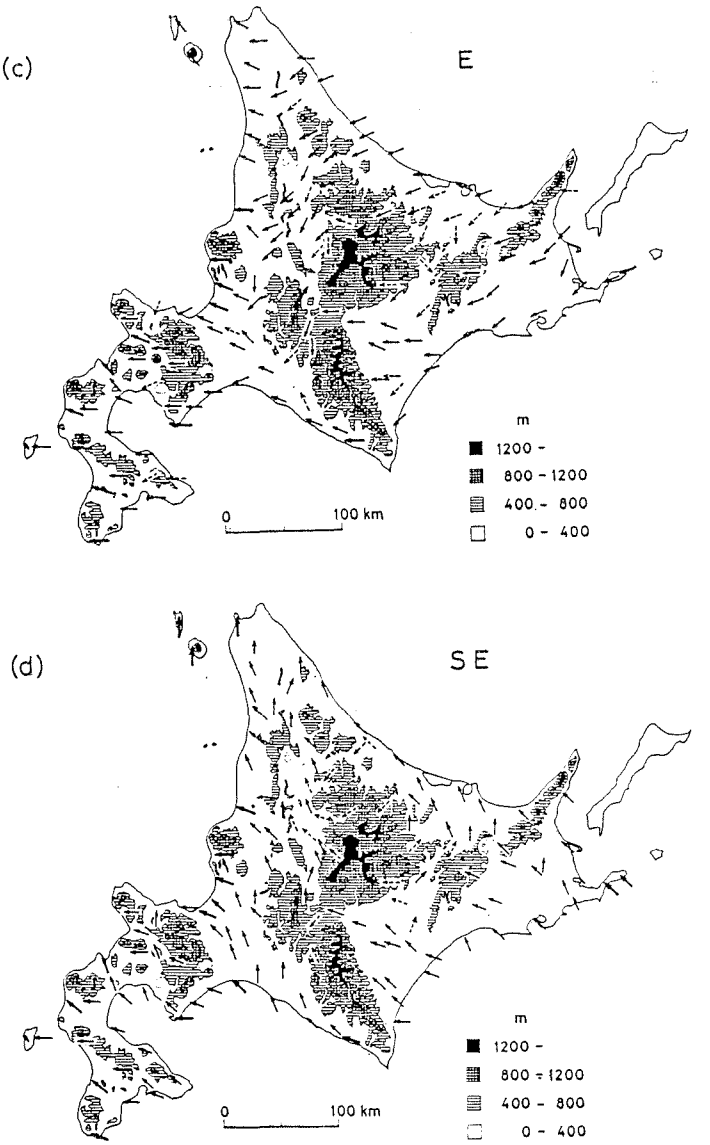

Fig. 5. (c)-(d) Same as (a), except for easterly and southeasterly general wind, respectively.

form an obstacle in the case of general winds.

The wind directions in the center or south of Ishikari Lowland change for about 90 degrees as the general wind turns from W to NW, although those in the northern area show hardly any change (see Figs. 5 (g) and (h)). This fact can explain a part of the phenomenon shown by Owada and Yoshino (1971), in which the surface wind directions of southern area of Ishikari Lowland are unstable in winter.

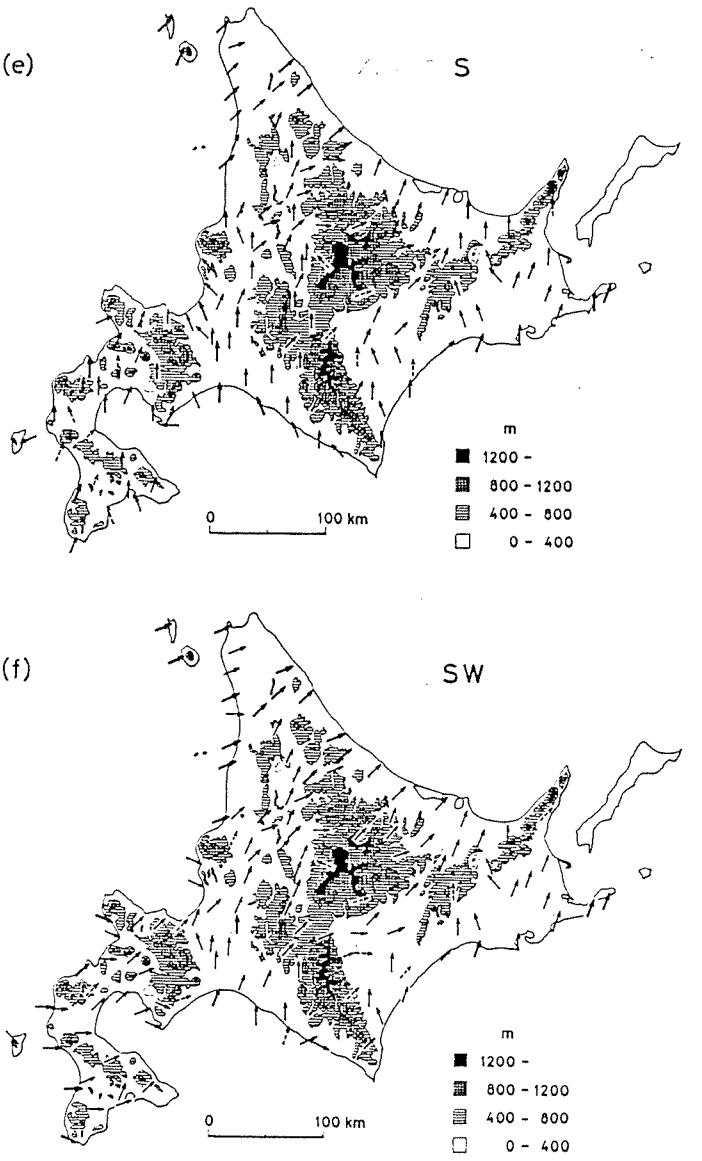

Fig. 5. (e)-(f) Same as (a), except for southerly and southwesterly general wind, respectively.

2) Eastern Pacific side and Abashiri District

Under the southerly wind system, the feature in which the stream lines are bent to NE by the Akan-Shiretoko Mountains corresponds to the report by Owada (1973). Furthermore, southerly wind seems to blow through the two mountain ranges (Fig. 5 (e)). Under the westerly flow (Fig. 5 (g)) the wind tends to blow along the mountains to the north of the southeastern side of Hokkaido.

Near Rausu, on the east of Shiretoko Peninsula, it is clear that the wind speed increases under the westerly or northwesterly general wind. The strong wind blow-

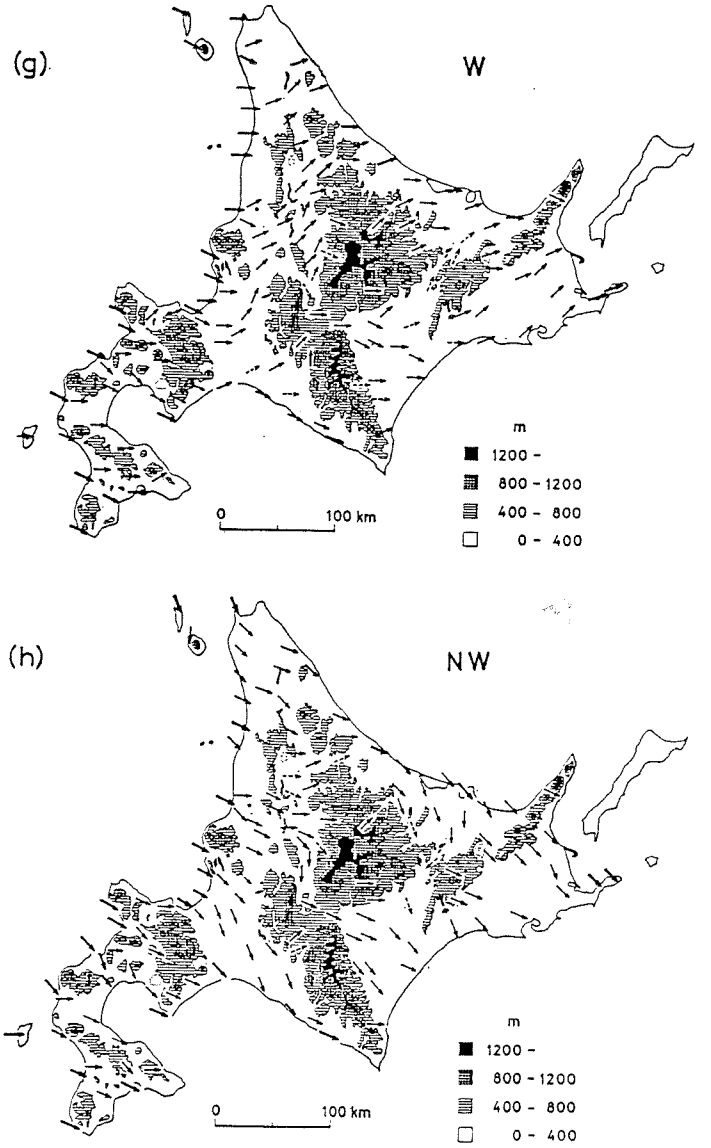

Fig. 5. (g)-(h) Same as (a), except for westerly and northwesterly general wind, respectively.

ing here is referred to as "Rausu-Kaze" by Arakawa (1969, 1971). Although the wind occurs under particular weather condition, the topography is assumed to be suitable for the generation of strong wind under these general wind directions (see Figs. 5 (g) and (h)).

On the Okhotsk Sea side near Abashiri, the southerly or northerly wind is relatively strong and the stream line seems to be clear in the case of these strong wind. These results are used for the explanation of the southerly strong wind studied by Yoshino *et al.* (1972). However, at Mombetsu, west-northwest of Abashiri, the wind speed increases when the general wind becomes westerly or easterly. It

is suggested that the wind system (air current system) changes in this vicinity.

3) Tokachi District

As discussed in the previous paper, (Kato, 1982), the features of westerly flow, in particular in the Tokachi Plain also exist clearly in the figures (Fig. 5(g)). Especially, it is interesting that the main flow toward the convergence zone near Karikachi Pass changes from southerly to northerly as the general wind direction varies from W to NW.

The features of Hidaka-Shimokaze reported by Arakawa (1969, 1971) are not marked clearly except for the convergence stream line near Urakwa, on the southwest of the Hidaka Mountains (Figs. 5(c) and (d)), because the area of such strong winds is small both in space and in time.

4) Kuromatsunai Lowland

The annual mean wind speed at Suttsu, to the north of Kuromatsunai Lowland, is the strongest in Hokkaido, and Tanaka (1958) showed that the wind speed increases especially under the southerly general wind here. From the figures such features are clearly marked, and furthermore, the strong winds are also recognized under the northerly general winds. These results show the funneling effect of the topography.

As mentioned above, the wind distribution patterns or the features of air currents are clarified by this analysis. It is one of the outstanding features of this method because the wind patterns are obtained for all directions of general winds.

b. Regional Characteristics of Air Current

Table 4 shows the wind speed at 22 meteorological stations when the general wind speed has maximal values throughout the year for each direction. For each station these values are normalized with the maximum wind speed corresponding to 10. In the table the normalized values less than 6 are shown by "–", and are regarded as weak wind speed. In other words, this table shows the general wind direction when a strong surface wind occurs at each station. To examine these results, the first five maximum wind speeds are selected from the daily data of 1979 and 1980, i. e. the total is 10 cases, for each station. The corresponding general wind directions for each case are shown by circles in Table 4. Thick solid circle indicates that the strong wind occurred more than two times in that general wind direction.

At all stations these strong winds tend to occur under the general wind direction at which the normalized surface wind speed is more than 7, and this table seems to show the actual cases. Although the result at Wakkanai has some errors, it depends on the fact shown by Narita and Masuyama (1955) that the surface wind changes by the force of pressure gradient even if the direction of the pressure gradient remains unchanged. Hence it is interesting to note that the results of Table 4 also closely resemble the figures for the probability of excess of wind speed for each station shown by Murakami *et al.* (1979).

Table 4. Calculated wind speed for each general wind direction on 22 meteorological stations when the general wind speed has the maximum value (presumed) for each direction during 1978. For each station the values are normalized as the maximum wind speed corresponds to 10, and the values less than 6 are shown by "—". Circles indicate the general wind directions corresponding to the first five maximum wind speeds (daily data) for each station both in 1979 and 1980. Squares shows that the strong wind occurred more than two times at that general wind direction

	GENERAL WIND DIRECTION															
	1	2	3	4	5	6	7	8	9	10	11	12	13	14	15	16
WAKKANAI	[7]	7	—	—	—	—	8	10	9	9	7	—	—	[—]	[8]	[8]
KITAMI E.	[7]	⑦	⊖	—	—	—	7	9	9	⑩	[8]	—	—	[—]	—	7
ASAHIKAWA	—	7	—	—	—	—	—	[7]	9	10	[10]	[8]	7	[—]	—	—
HABORO	—	—	—	—	—	—	7	8	9	10	⑨	[8]	[8]	[7]	—	—
SAPPORO	—	—	—	—	8	9	⑩	[8]	⊖	—	—	—	8	⑨	⑨	⑦
IWAMIZAWA	8	[—]	—	⊖	—	7	8	[10]	9	[8]	⑦	—	—	⊖	—	8
OTARU	⊖	—	—	—	—	—	—	—	—	—	[8]	⑩	9	[9]	⑦	⊖
KUTCHAN	—	—	—	—	—	⑦	8	8	8	7	[7]	⑧	9	[10]	10	8
SUTTSU	—	—	—	—	8	[9]	⑩	[8]	—	—	—	—	9	[9]	9	⑧
OHMU	—	—	—	—	—	—	—	7	7	9	[10]	[9]	⑧	[7]	—	—
MOMBETSU	—	—	—	—	—	—	—	—	—	—	8	9	⑩	[9]	⑦	[—]
ABASHIRI	⑧	7	—	—	—	7	9	⑨	9	7	—	—	7	[9]	[10]	[9]
NEMURO	⑧	8	7	—	7	8	9	⑨	9	8	8	8	9	[9]	[10]	[9]
KUSHIRO	[10]	[9]	7	—	—	—	8	9	9	9	⑦	—	[—]	[—]	8	9
OBIHIRO	—	—	—	—	—	7	—	—	—	—	—	8	9	[10]	[9]	⊖
HIROO	7	⊖	—	—	—	—	—	—	—	7	[9]	[10]	⑩	[10]	8	7
TOMAKOMAI	⑧	⑦	⊖	—	—	⑦	⑨	[9]	9	⑦	[—]	—	—	8	9	10
MURORAN	—	—	—	7	7	7	—	—	—	—	—	⑨	[10]	[9]	8	—
URAKAWA	—	—	—	7	7	7	—	—	—	—	⊖	[9]	[10]	[9]	8	—
OSHAMANBE	⊖	—	—	—	—	[7]	⑦	⊖	—	—	⊖	⊖	8	9	10	[8]
HAKODATE	—	—	—	—	⑦	[7]	⊖	—	—	⊖	[7]	⑨	10	⑩	8	—
ESASHI	—	—	—	—	—	—	—	—	—	⑦	[8]	[9]	⑩	[9]	8	⊖

Since the results represented in Table 4 seem to express the regional characteristics of wind, these values are used for the cluster analysis to determine the regions with similar features of wind. Three clustering regions are shown in Fig. 6 (a). Averaged features of wind variation for each group are shown in Fig. 6 (b), i. e., the wind speed increases when the general wind direction is about 1) S or N for the group I, 2) SW or NE for the group II, and 3) NW or SE for the group III, respectively. It is worthy of note that the boundary of wind variation type between two groups exists in the north of Ishikari Plain which was also revealed in the previous paper (Kato, 1982). Furthermore, the other boundary of wind variation type is clearly marked near Mombetsu which is also noted in the

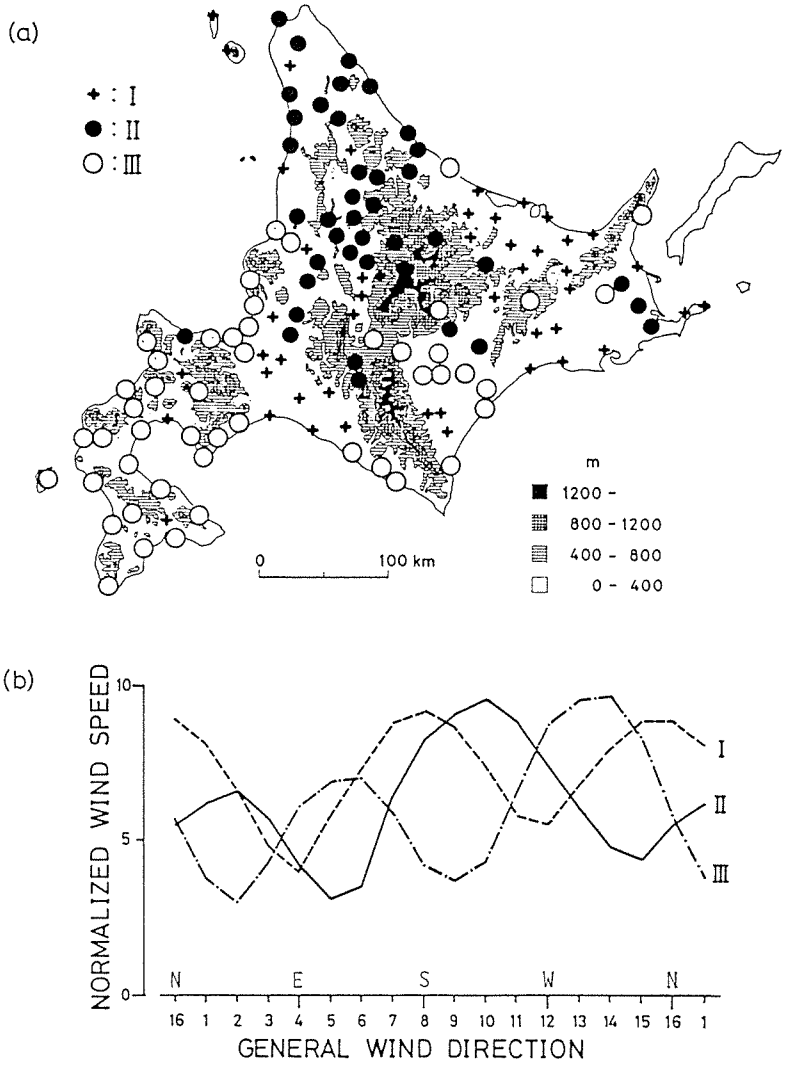

Fig. 6. (a) Regionalization depending upon the clustering of the calculated wind speed for each general wind direction, and (b) the characteristics of wind variation for each group. See the text for detail.

previous section.

Indeed Fig. 6 closely resembles Fig. 7 of Kato (1982) in spite of the difference of the method. This fact indicates that each area with homogeneous regionality of wind variation type exist, for example, Ishikari Plain, Kamikawa Basin, Kuromatsunai Lowland and so on, although the boundaries are not clear in many cases. These results will be used not only for the explanation of the distribution pattern of the other climatic elements but also for the study of wind energy, for example in reported by Komine *et al.* (1980).

5. Conclusions

In order to clarify the various features of air current systems, AMeDAS data are analysed by means of the original method using PCA. The air current maps obtained in this study correspond to the wind pattern when the general wind speed in each direction has the annual maximum value, and reflect the actual wind patterns. From these results, the structure and the extension of the air currents for each general wind direction were revealed.

Using the calculated wind speed at the stations for each general wind direction, the regionality of wind was clarified by means of cluster analysis. The boundaries (transitional zones) of the wind variation type agree with the limitation of the extent of some air currents.

The regional characteristics of air current system in Hokkaido are mainly governed by the speed of westerly general winds. Secondly characteristics depend on the fact that the topography surrounding the region is suitable for generating the strong air current under the southeasterly or the southwesterly general winds. Such characteristics agree well with the previous study (Kato, 1982).

By these methods, wind distribution patterns determined by synoptic scale pressure field and the major topographical features alone can be delineated, and the noise such as background fluctuation of wind peculiar to each station or the wind related to the heat effect are removed. This is the outstanding merit of these methods.

Hereafter, it is necessary to investigate the wind pattern under the weak pressure gradient, i. e., the wind pattern depend on the heat effect. Furthermore, these methods may be applied to the other regions, and the propriety of the results should be also examined.

Acknowledgements

The author wishes to thank Prof. Hiroshi Kadomura, Graduate School of Environmental Science, Hokkaido University, for his helpful suggestions, encouragement and guidance in the course of this work. The author also wishes to thank Assoc. Prof. Hidenori Takahashi, Graduate School of Environmental Science, Hokkaido University, for his helpful discussion and advice. Special thanks is also given to Prof. Katsuhiro Kikuchi, Department of Geophysics, Hokkaido University, for his friendly advice. The author must not forget the assistance from the sections of Japan Meteorological Agency for supplying the AMeDAS data tapes.

This paper is a part of the doctoral dissertation submited to Hokkaido University. Numerical computation was done at the Hokkaido University Computing Center. The original data were compiled at Tokyo University Computing Center.

References

Arakawa, S. (1969): Climatological and dynamical studies on the local strong winds, mainly in Hokkaido, Japan. *Geophys. Mag.*, **34**, 359–425.

Arakawa, S. (1971): On the local strong winds. *Tenki*, **18**, 103–115*.

Barnett, T. P. (1977): The principal time and space scales of the Pacific trade wind fields. *J. Atmos. Sci.*, **34**, 221–236.

Enfield, D. B. (1981): Annual and nonseasonal variability of monthly low-level wind fields over the Southeastern Tropical Pacific. *Mon. Wea. Rev.*, **109**, 2177–2190.

Hardy, D. M. (1978): Principal components analysis of vector wind measurements. *J. Appl. Meteor.*, **17**, 1153–1162.

Kato, H. (1982): Regionality of surface wind in Hokkaido: An analysis by means of PCA. *Environ. Sci., Hokkaido*, **5** (2), 293–304**.

Kawamura, T. (1963): Surface wind distribution in Hokkaido in winter. *J. Met. Res.*, **15**, 533–537**.

Kawamura, T. (1966): Surface wind system over central Japan in the winter season. *Geogr. Rev. Japan*, **39**, 538–554**.

Komine, H., Murakami, S., Shibata, H. and Matsuno, N. (1980): Prediction of surface wind velocity at any point, using regression analysis of topographic effects on wind velocity. *Tenki*, **27**, 849–861*.

Murakami, S. (1979): *The study on the geographical distribution and the seasonal variation of wind energy in Japan.* Committee of Study on the Geographical Distribution and the Seasonal Variation of Wind Energy in Japan, 163 p*.

Narita, G. and Masuyama, R. (1955): On the influence of topography upon the wind direction at Wakkanai. *J. Met. Res.*, **7**, 797–799*.

Owada, M. and Yoshino, M. M. (1971): Prevailing winds in the Ishikari Plain, Hokkaido. *Geogr. Rev. Japan*, **44**, 638–652**.

Owada, M. (1973): Prevailing winds in the Konsen-Genya, Southeastern Hokkaido. *Geogr. Rev. Japan*, **46**, 505–515**.

Tanaka, T. (1958): Some characters of gale in Suttsu District, Hokkaido. *J. Met. Res.*, **10**, 596–602*.

Wakamatsu, S. and Hatano, S. (1981): Local wind analysis using P. C. A.. *J. Japan Soc. Air Pollut.*, **16**, 379–386**.

Yoshino, M. M., Hoshino, M. and Owada, M. (1972): On the local wind distribution and the wind break density in the Shari-Abashiri region, Hokkaido. *J. Agr. Met. Japan*, **27**, 145–152.

* in Japanese.

** in Japanese with English abstract.

Abstract

In order to clarify the various features of air current systems, AMeDAS data are analysed by means of an original method using PCA. The air currents shown on the maps correspond to the wind patterns when the general wind speed in each direction has the annual maximum value, and reflect the actual wind patterns. From these results, the structure and the extension of the air currents for each general wind direction were revealed.

The regional characteristics of air current system (wind variation type) in Hokkaido are mainly governed by the speed of westerly general winds. Secondary characteristics depend on the fact that the topography surrounding the region is suitable for generating the strong air current under the southeasterly or the southwesterly general winds.